

Differentiable Sorting Networks for Scalable Sorting and Ranking Supervision

Felix Petersen¹ Christian Borgelt² Hilde Kuehne^{3,4} Oliver Deussen¹

Abstract

Sorting and ranking supervision is a method for training neural networks end-to-end based on ordering constraints. That is, the ground truth order of sets of samples is known, while their absolute values remain unsupervised. For that, we propose differentiable sorting networks by relaxing their pairwise conditional swap operations. To address the problems of vanishing gradients and extensive blurring that arise with larger numbers of layers, we propose mapping activations to regions with moderate gradients. We consider odd-even as well as bitonic sorting networks, which outperform existing relaxations of the sorting operation. We show that bitonic sorting networks can achieve stable training on large input sets of up to 1024 elements.

1. Introduction

Sorting and ranking as the ability to score elements by their relevance is an essential task in numerous applications. It can be used for choosing the best results to display by a search engine or organize data in memory. Starting in the 1950s, sorting networks have been presented to address the sorting task (Knuth, 1998). Sorting networks are sorting algorithms with a fixed execution structure, which makes them suitable for hardware implementations, e.g., as part of circuit designs. They are oblivious to the input, i.e., their execution structure is independent of the data to be sorted. As such hardware implementations are significantly faster than conventional multi-purpose hardware, they are of interest for sorting in high performance computing applications (Govindaraju et al., 2006). This motivated the optimization of sorting networks toward faster networks with fewer layers, which is a still-standing problem (Bidlo & Dobeš, 2019). Note that, although the name is similar, sorting networks are *not* neural networks that perform sorting.

¹University of Konstanz, Germany ²University of Salzburg, Austria ³University of Frankfurt, Germany ⁴MIT-IBM Watson AI Lab. Correspondence to: Felix Petersen <felix.petersen@uni.kn>.

Recently, the idea of end-to-end training of neural networks with sorting and ranking supervision by a continuous relaxation of the sorting and ranking functions has been presented by Grover et al. (2019). Sorting supervision means the ground truth order of some samples is known while their absolute values remain unsupervised. As the error has to be propagated in a meaningful way back to the neural network, it is necessary to use a continuous and continuously differentiable sorting function. Several such differentiable relaxations of the sorting and ranking functions have been introduced, e.g., by Grover et al. (2019), Cuturi et al. (2019), and Blondel et al. (2020). For example, this allows training a CNN based on ordering and ranking information instead of absolute ground truth values. As sorting a sequence of values requires finding the respective ranking order, we use the terms “sorting” and “ranking” interchangeably.

In this work, we propose to combine traditional sorting networks and differentiable sorting functions by presenting smooth differentiable sorting networks.

Sorting networks are conventionally non-differentiable as they use min and max operators for conditionally swapping elements. Thus, we relax these operators by building on the softmax and softmax operators. However, due to the nature of the sorting network, values with large as well as very small differences are compared in each layer. Comparing values with large differences causes vanishing gradients, while comparing values with very small differences can modify, i.e., blur, values as they are only partially swapped. This is because softmax and softmax are based on the logistic function which is saturated for large inputs but also returns a value close to the mean for inputs that are close to each other. Based on these observations, we propose an activation replacement trick, which avoids vanishing gradients as well as blurring. That is, we modify the distribution of the differences between compared values to avoid small differences close to 0 as well as large differences.

To validate the proposed idea and to show its generalization, we evaluate two sorting network architectures, the odd-even as well as the bitonic sorting network. The idea of odd-even sort is to iteratively compare adjacent elements and swap pairs that are in the wrong order. The method alternately compares all elements at odd and even indices with their successors. To make sure that the smallest (or greatest) ele-

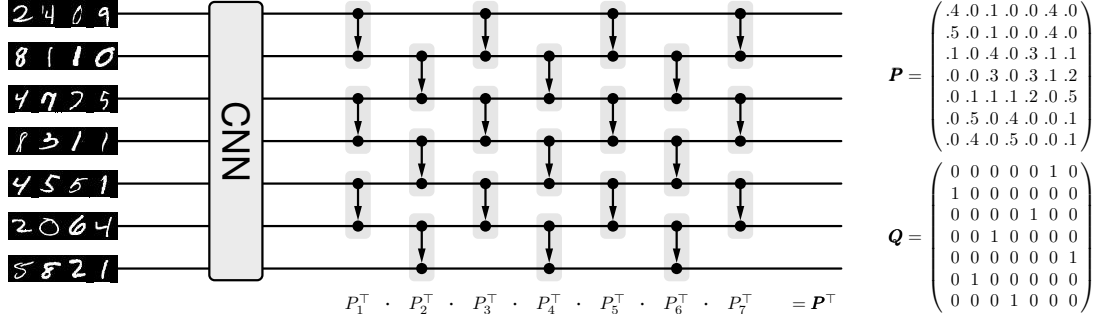


Figure 1: Overview of the system for training with sorting supervision. Left: input images are fed separately / independently into a Convolutional Neural Network (CNN) that maps them to scalar values. Center: the odd-even sorting network sorts the scalars by parallel conditional swap operations. Right: the sorting network produces a differentiable permutation matrix P which can then be compared to the ground truth permutation matrix Q using binary cross-entropy to produce the training loss. By propagating this error backward through the sorting network, we can train the CNN.

ment will be propagated to its final position for any possible input of length n , we need n exchange layers. An odd-even sorting network is displayed in Figure 1 (center). Odd-even networks can be seen as the most generic architectures, and are mainly suitable for smaller input sets as their number of layers directly depends on this factor.

Bitonic sorting networks (Batcher, 1968) use bitonic sequences to sort based on the Divide-and-Conquer principle and allow sorting within only $\mathcal{O}(\log^2 n)$ parallel time. Bitonic sequences are twice monotonic sequences, i.e., they consist of a monotonically increasing and monotonically decreasing sequence. Bitonic sorting networks recursively combine pairs of monotonic sequences into bitonic sequences and then merge them into single monotonic sequences. Starting at single elements, they eventually end up with one sorted monotonic sequence. With the bitonic architecture, we can sort large numbers of input values as we only need $\frac{\log_2 n \cdot (\log_2 n + 1)}{2}$ layers to sort n inputs. As a consequence, the proposed architecture provides good accuracy even for large input sets and allows scaling up sorting and ranking supervision to large input sets with up to 1024 elements.

Following Grover et al. (2019) and Cuturi et al. (2019), we benchmark our continuous relaxation of the sorting function on the four-digit MNIST (LeCun et al., 2010) sorting supervision benchmark. To evaluate the performance in the context of a real-world application, we apply our continuous relaxation to the multi-digit images of the Street View House Number (SVHN) data set. We compare the performance of both sorting network architectures and evaluate their characteristics under different conditions. We show that both differentiable sorting network architectures outperform existing continuous relaxations of the sorting function on the four-digit MNIST sorting benchmark and also perform well on the more realistic SVHN benchmark. Further,

we show that our model scales and achieves performance gains on larger sets of ordered elements and confirm this up to $n = 1024$ elements.

An overview of the overall architecture is shown in Figure 1.

2. Related work

Sorting Networks. The goal of research on sorting networks is to find optimal sorting networks, i.e., networks that can sort an input of n elements in as few layers of parallel swap operations as possible. Initial attempts to sorting networks required $\mathcal{O}(n)$ layers, each of which requires $\mathcal{O}(n)$ operations (examples are bubble and insertion sort (Knuth, 1998)). With parallel hardware, these sorting algorithms can be executed in $\mathcal{O}(n)$ time. Further research lead to the discovery of the bitonic sorting network (aka. bitonic sorter) which requires only $\mathcal{O}(\log^2 n)$ layers (Knuth, 1998; Batcher, 1968). Using genetic and evolutionary algorithms, slightly better optimal sorting networks were found for specific n (Bidlo & Dobeš, 2019; Baddar & Batcher, 2012). However, these networks do not exhibit a simple, regular structure. Ajtai, Komlós, and Szemerédi (Ajtai et al., 1983) presented the AKS sorting network which can sort in $\mathcal{O}(\log n)$ parallel time, i.e., using only $\mathcal{O}(n \log n)$ operations. However, the complexity constants for the AKS algorithm are to date unknown and optimistic approximations assume that it is faster than bitonic sort if and only if $n \gg 10^{80}$. Today, sorting networks are still in use, e.g., for fast sorting implementations on GPU accelerated hardware as described by Govindaraju et al. (2006) and in hybrid systems as described by Gowinlock & Karsin (2019).

In the past, various approaches combining neural networks and sorting have been proposed. The idea of integrating the bitonic sorting network into a neural network architecture has been discussed, e.g., by Ceterchi & Tomescu (2008) in the context of spiking neural P systems. These systems are

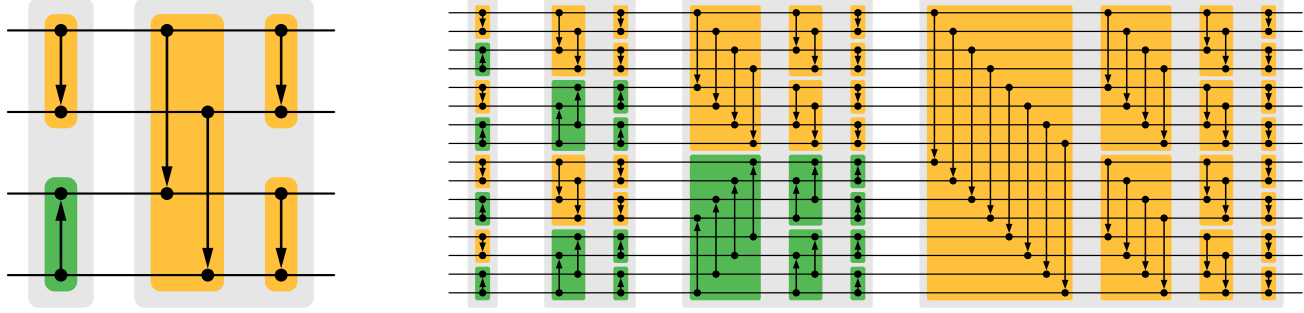


Figure 2: Bitonic sorting networks for 4 and 16 lanes, consisting of bitonic merge blocks (colored).

predecessors of current spiking networks, a form of computational models inspired by biological neurons. Ceterchi & Tomescu (2008) propose a theoretical formulation how a bitonic sorting network could be integrated into spiking neural P systems. The idea was later adapted by Metta & Kelemenova (2015) for a spiking neural P system with anti-spikes and rules on synapses. They use the bitonic as well as the bead sort algorithm to evaluate the characteristics of the proposed activation ideas. Based on the bitonic sorting network Lim & Wright (2016) propose a coordinate descent algorithm to solve hard permutation problems.

Neural Networks with Sorting Supervision. Closest to the work proposed here are approaches that train a neural network based on sorting and ranking supervision. Grover et al. (2019) consider pairwise distances between elements to develop NeuralSort. They propose a continuous relaxation of permutation matrices to the set of unimodal row-stochastic matrices. For evaluation, they propose the benchmark of predicting the scalar value displayed on concatenated four-digit MNIST numbers. As supervision, they use the ranking of between 3 and 15 of those numbers.

Following this work, Cuturi et al. (2019) presented a method for smoothed ranking and sorting operators using optimal transport (OT). They use the idea that sorting can be achieved by minimizing the matching cost between elements and an auxiliary target of increasing values. That is, the smallest element is matched to the first value, the second smallest to the second value, etc. They make this differentiable by regularizing the OT problem with an entropic penalty and solving it by applying Sinkhorn iterations. Based on this idea, Xie et al. (2020) have used OT to devise a differentiable top- k operator for image classification and differentiable beam search.

Recently, Blondel et al. (2020) presented the idea of constructing differentiable sorting and ranking operators as projections onto the permutohedron as the convex hull of permutations. They solve this by reducing it to isotonic optimization and make it differentiable by considering the Jacobians of the isotonic optimization and the projection.

3. Sorting Networks

3.1. Odd-Even Sorting Network

One of the simplest sorting networks is the fully connected odd-even sorting network. Here, neighboring elements are swapped if they are in the wrong order. As the name implies, this is done in a fashion alternating between comparing odd and even indexed elements with their successor. In detail, for sorting an input sequence $a_1 a_2 \dots a_n$, each layer updates the elements such that $a'_i = \min(a_i, a_{i+1})$ and $a'_{i+1} = \max(a_i, a_{i+1})$ for all odd or even indices i , respectively. Using n of such layers, a sequence of n elements is sorted as displayed in Figure 1 (center).

3.2. Bitonic Sorting Network

Second, we review the bitonic sorting network for sorting $n = 2^k$ elements where $k \in \mathbb{N}_+$. If desired, the sorting network can be extended to $n \in \mathbb{N}_+$ (Knuth, 1998).

In general, a sequence $(a_i)_{1 \leq i < n}$ is bitonic if (after an appropriate circular shift) $a_1 \leq \dots \leq a_j \geq \dots \geq a_n$ for some j , $1 \leq j \leq n$. Such a bitonic sequence is sketched in Figure 3a (top).

Following the Divide-and-Conquer principle, in analogy to merge sort, bitonic sort recursively splits the task of sorting a sequence into the tasks of sorting two subsequences of equal length, which are then merged. Like merge sort, bitonic sort starts by merging single element lists, to obtain sorted lists of length 2, but alternating between non-decreasing and non-increasing order (first gray block in Figure 2). Pairs of these are merged into monotonic sequences, again alternating between non-decreasing and non-increasing order (second gray block in Figure 2). This proceeds, doubling the length of the sorted sequences with each (gray) block until the whole sequence is sorted. The difference to merge sort lies in the bitonic merge operation, which merges two sequences sorted in opposite order (i.e. a single bitonic sequence) into a single sorted (monotonic) sequence.

In detail, a bitonic sequence is sorted by several bitonic

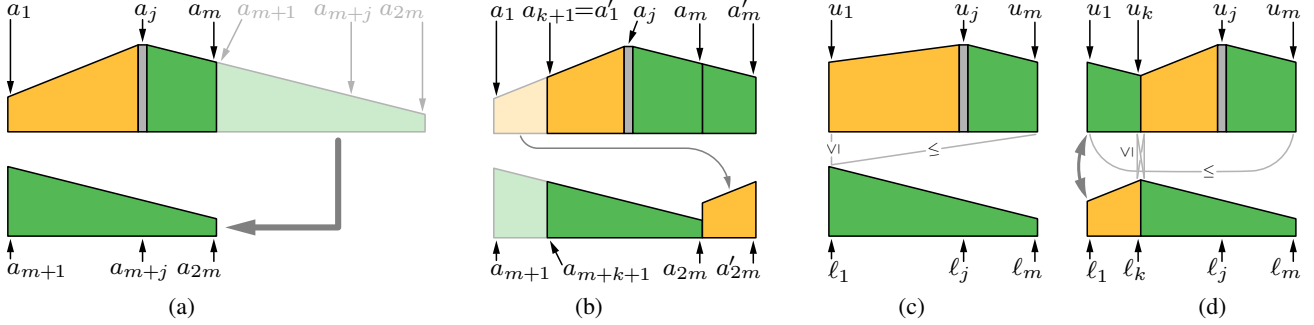


Figure 3: Bitonic merge turns a bitonic input sequence into two bitonic output sequences, with all elements in the one (upper, u_i) sequence larger than all elements in the other (lower, ℓ_i) sequence. The diagrams show the vertical alignment of elements to compare (a) and the invariance to cyclic permutations (b). Depending on the values in (a), no exchanges (c) or exchanges (d) are executed.

merge blocks, shown in orange and green in Figure 2. Each block takes a bitonic input sequence $a_1 a_2 \dots a_{2m}$ of length $2m$ and turns it into two bitonic output sequences $\ell_1 \ell_2 \dots \ell_m$ and $u_1 u_2 \dots u_m$ of length m that satisfy $\max_{i=1}^m \ell_i \leq \min_{i=1}^m u_i$. These subsequences are recursively processed by bitonic merge blocks, until the output sequences are of length 1. At this point, the initial bitonic sequence has been turned into a monotonic sequence due to the minimum/maximum conditions that hold between the output sequences (and thus elements).

A bitonic merge block computes its output as $\ell_i = \min(a_i, a_{m+i})$ and $u_i = \max(a_i, a_{m+i})$. This is depicted in Figure 2 by the arrows pointing from the minimum to the maximum. To demonstrate that bitonic merge works, we show that this operation indeed produces two bitonic output sequences for which the relationship $\max_{i=1}^m \ell_i \leq \min_{i=1}^m u_i$ holds.

Note that neither a cyclic permutation of the sequence ($a'_i = a_{(i+k-1 \bmod 2m)+1}$ for some k , Figure 3b), nor a reversal, change the bitonic character of the sequence. As can be seen in Figure 3b, even under cyclic permutation still the same pairs of elements are considered for a potential swap. Thus, as a cyclic permutation or a reversal only causes the output sequences to be analogously cyclically permuted or reversed, this changes neither the bitonic character of these sequences nor the relationship between them. Therefore, it suffices to consider the special case shown in Figure 3a, with a monotonically increasing sequence (orange) followed by a monotonically decreasing sequence (green) and the maximum element a_j (gray) in the first half. Note that in this case $\forall i; j \leq i \leq m : a_i \geq a_{m+i} \wedge u_i = a_i \wedge \ell_i = a_{m+i}$.

For this case, we have to distinguish two sub-cases:

$a_1 \geq a_{m+1}$ and $a_1 < a_{m+1}$.

If, on one hand, $a_1 \geq a_{m+1}$, we have the situation shown in Figure 3c: the output sequence $u_1 u_2 \dots u_m$ is simply the

first half of the sequence, the output sequence $\ell_1 \ell_2 \dots \ell_m$ is the second half. Thus, both output sequences are bitonic (since they are subsequences of a bitonic input sequence) and $\min_{i=1}^m u_i = \min(u_1, u_m) \geq \ell_1 = \max_{i=1}^m \ell_i$.

If, on the other hand, $a_1 < a_{m+1}$, we can infer $\exists k; 1 \leq k < j : a_k > a_{m+k} \wedge a_{k+1} \leq a_{m+k+1}$. This situation is depicted in Figure 3d. Thus, $\forall i; 1 \leq i \leq k : u_i = a_{m+i} \wedge \ell_i = a_i$ and $\forall i; k < i \leq m : u_i = a_i \wedge \ell_i = a_{m+i}$. Since $u_k = a_{m+k} > a_k = \ell_k$, $u_{k+1} = a_{m+k+1} \geq a_{m+k+1} = \ell_{k+1}$, $u_{k+1} = a_{k+1} \geq a_k = \ell_k$, we obtain $\max_{i=1}^m \ell_i \leq \min_{i=1}^m u_i$. Figure 3d shows that the two output sequences are bitonic and that all elements of the upper output sequence are greater than or equal to all elements of the lower output sequence.

4. Differentiable Sorting Networks

We use softmax and softmax to define the relaxations of the min and max operators, which are used as a basis for the swap operations in sorting networks. Therefore, our formulation is based on the logistic sigmoid function $\sigma(x) = \frac{1}{1+e^{-x}}$. For a_i, a_j , we define in accordance to softmax and softmax

$$\min_{\sigma, s}(a_i, a_j) := \alpha_{ij} \cdot a_i + (1 - \alpha_{ij}) \cdot a_j \quad (1)$$

$$\max_{\sigma, s}(a_i, a_j) := (1 - \alpha_{ij}) \cdot a_i + \alpha_{ij} \cdot a_j \quad (2)$$

where

$$\alpha_{ij} := \sigma((a_j - a_i) \cdot s). \quad (3)$$

Here, s denotes a steepness hyperparameter such that for $s \rightarrow \infty$ the smooth operators converges to the discrete operators. As we show in the next section, it is necessary to extend this formulation by the activation replacement trick φ .

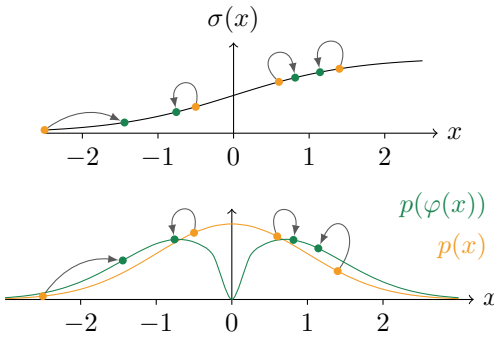


Figure 4: Top: the logistic sigmoid function where the input values x (orange) are mapped to $\varphi(x)$ (green) and thus being closer to -1 and $+1$. Bottom: probability density functions of Gaussian distributed values x (orange) and the distribution of values $\varphi(x)$ (green).

4.1. Activation Replacement Trick φ

Assuming that the inputs to a sorting network are normally distributed, there are many cases in which the differences of two values $|a_j - a_i|$ are very small as well as many cases in which the differences are very large. For the relaxation of sorting networks, this poses two problems:

If $|a_j - a_i|$ is close to 0, while we obtain large gradients, this also blurs the two values to a great extent, modifying them considerably. Thus, it is desirable to avoid $|a_j - a_i| \approx 0$.

On the other hand, if $|a_j - a_i|$ is large, vanishing gradient occur, which hinders training.

To counter these two problems at the same time, we propose the activation replacement trick. We transform the differences between two values to be potentially swapped (e.g., $x = (a_j - a_i)$) from a unimodal distribution (which is similar to a Gaussian distribution) into a bimodal distribution which has a low probability density around 0. To this end, we apply the transformation

$$\varphi : x \mapsto \frac{x}{|x|^\alpha + \epsilon} \quad (4)$$

to the differences x , where $\alpha \in [0, 1]$ and $\epsilon \approx 10^{-10}$. φ pushes all values (depending on the sign) toward -1 and $+1$, respectively. Thus, by applying φ before σ , we move the values outside $[-1, +1]$ to positions at which they have a greater gradient, thus mitigating vanishing gradients. Simultaneously, we achieve a probability density of 0 at $|a_j - a_i| = 0$ ($p(\varphi(0)) = 0$) as all values close to zero are mapped toward -1 and $+1$, respectively. This is displayed in Figure 4.

As we multiply by the steepness parameter s (Equation 3), we map the input to the sigmoid function toward $-s$ and $+s$, respectively. Thus, when replacing $\sigma(x \cdot s)$ by $\sigma(\varphi(x) \cdot s)$,

we push the output values toward $\frac{1}{1+e^{-1 \cdot s}}$ or $\frac{1}{1+e^{1 \cdot s}}$. This increases the gradient $\frac{\partial \sigma(\varphi(x) \cdot s)}{\partial x}$ for all $x \in \mathbb{R} \setminus [-1, +1]$ which are those values causing the vanishing gradients, addressing the problem of vanishing gradients. Further, for all $x \in [-1, +1]$ this pushes the output values away from $\frac{1}{2}$, addressing the problem of blurring of values.

Therefore, we extend our formulation of the relaxations of the min and max operators by defining

$$\alpha_{ij} := \sigma(\varphi(a_j - a_i) \cdot s). \quad (5)$$

Empirically, the activation replacement trick accelerates the training through our sorting network. We observe that, while sorting networks up to 21 layers, i.e., bitonic networks with $n \leq 64$, can operate with moderate steepness (i.e., $s \leq 15$) and without the activation replacement trick (i.e., $\alpha = 0$), for more layers, the activation replacement trick becomes necessary for good performance. Notably, the activation replacement trick also improves the performance for sorting networks with fewer layers. Further, the activation replacement trick allows training with smaller steepness s , which makes training more stable specifically for long sequences as it avoids exploding gradients.

Note that, in case of bitonic, in the first layer of the last merge block, $n/2$ elements in non-descending order are element-wise compared to $n/2$ elements in non-ascending order. Thus, in this layer, we compare the minimum of the first sequence to the maximum of the second sequence and vice versa. At the same time, we also compare the median of both sequences as well as values close to the median to each other. As we consider very large differences as well as very small differences in the same layer, the activation replacement trick achieves an equalization of the mixing behavior, which reduces blurring.

4.2. Differentiable Permutation Matrices

For sorting and ranking supervision, i.e., training a neural network to predict scalars, where only the order of these scalars is known, we use the ground truth permutation matrix as supervision. Thus, to train an underlying neural network end-to-end through the differentiable sorting network, we need to return the underlying permutation matrix rather than the actual sorted scalar values. For that, we compute the permutation matrices for the swap operations for each layer as shown in Figure 1. Here, for all swap operations between any elements a_i and a_j that are to be ordered in non-descending order, the layer-wise permutation matrix is

$$P_{l,ii} = P_{l,jj} := \sigma(\varphi(a_j - a_i) \cdot s), \quad (6)$$

$$P_{l,ij} = P_{l,ji} := 1 - \sigma(\varphi(a_j - a_i) \cdot s) \quad (7)$$

where all other entries of P_l set to 0. By multiplication, we can compute the complete relaxed permutation matrix \mathbf{P} as

$$\mathbf{P} = P_n \cdot \dots \cdot P_2 \cdot P_1 = \left(\prod_{l=1}^n P_l^\top \right)^\top. \quad (8)$$

A column in the relaxed permutation matrix can be seen as a distribution over possible ranks for the corresponding input value. Given a ground truth permutation matrix \mathbf{Q} , we can define our column-wise cross entropy loss as

$$\mathcal{L} := \sum_{c=1}^n \left(\frac{1}{n} \text{CE}(\mathbf{P}_c, \mathbf{Q}_c) \right) \quad (9)$$

where \mathbf{P}_c and \mathbf{Q}_c denote the c th columns of \mathbf{P} \mathbf{Q} , respectively. Note that, as the cross entropy loss is, by definition, computed element-wise, the column-wise cross entropy is equivalent to the row-wise cross entropy.

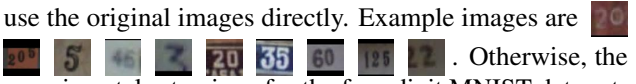
5. Experiments

We evaluate the proposed differentiable sorting networks on the four-digit MNIST sorting benchmark (Grover et al., 2019; Cuturi et al., 2019) as well as on the real-world SVHN data set.¹

MNIST For the four-digit MNIST sorting benchmark, MNIST digits are concatenated to four-digit numbers, e.g.,  A CNN then predicts a scalar value corresponding to the value displayed on the four-digit image. For training, n of those four-digit images are separately processed by the CNN and then sorted by the relaxed sorting network as shown in Figure 1. Based on the permutation matrix produced by the sorting network and the ground truth ranking, the training objective is computed (Equation 9) and the CNN is updated. At test time, we forward single images of four-digit numbers from the test data set. For evaluation, the discrete rankings of the predicted values are compared to the rankings of their ground truth. Note that the n used for test and evaluation can be independent of the n used for training.

SVHN Since the multi-digit MNIST data set is an artificial data set, we also evaluate our technique on the SVHN data set (Netzer et al., 2011). This data set comprises house numbers collected from Google Street View and provides a larger variety wrt. different fonts and formats than the MNIST data set. We use the published “Format 1” and preprocess it as described by Goodfellow et al. (2013), cropping the centered multi-digit numbers with a boundary of 30%, resizing it to a resolution of 64×64 , and then selecting 54×54 pixels at a random location. As SVHN contains

¹Our PyTorch as well as a native CUDA implementation will be publicly available upon publication.

1 – 5 digit numbers, we can avoid the concatenation and use the original images directly. Example images are  . Otherwise, the experimental setup is as for the four-digit MNIST data set.

Network Architecture For the MNIST sorting task, we use the same convolutional neural network (CNN) architecture as Grover et al. (2019) and Cuturi et al. (2019) to allow for comparability. This architecture consists of two convolutional layers with a kernel size of 5×5 , 32 and 64 channels respectively, each followed by a ReLU and MaxPool layer; this is (after flattening) followed by a fully connected layer with a size of 64, a ReLU layer, and a fully connected output layer mapping to a scalar.

For the SVHN task, we use a network with four convolutional layers with a kernel size of 5×5 and (32, 64, 128, 256) filters, each followed by a ReLU and a max-pooling layer with stride 2×2 ; followed by a fully connected layer with size 64, a ReLU, and a layer with output size 1.

Evaluation Metrics For evaluation, discrete rankings based on the scalar predictions are computed and compared to the discrete ground truth rankings. As in previous works, we use the evaluation metrics of exact match (EM) of the predicted ranking, and fraction of element-wise correct ranks (EW) in the predicted ranking. For EM and EW, we follow Grover et al. (2019) and Cuturi et al. (2019), and use the same n for training and evaluation. However, this can be a problem in the context of large input sets as these evaluation metrics become unreliable as n increases. For example, the difficulty of exact matches rises with the factorial of n , which is why they become too sparse to allow for valid conclusions for large n . To allow for a comparison of the performance independent of the number of elements n used for training, we also evaluate the models based on the EM accuracy for $n = 5$ (EM5). That is, the network can be trained with an arbitrary n , but the evaluation is done for $n = 5$. A table with respective standard deviations can be found in the supplementary material.

Training Settings We use the Adam optimizer (Kingma & Ba, 2015) with a learning rate of $10^{-3.5}$, and up to 10^6 iterations of training. Furthermore, we set $\alpha = 0.25$ and a use a steepness of two times the number of layers ($s = 2n$ for odd-even and $s = (\log_2 n)(1 + \log_2 n)$ for bitonic.) We use a constant batch size of 100 as in previous works unless denoted otherwise. Note that, although α is chosen as a constant value for all n , a higher accuracy is possible when optimizing α for each n separately.

Comparison to State-of-the-Art (MNIST) We first compare our approach to the systems proposed by Grover et al. (2019) and Cuturi et al. (2019). Here, we follow the

Table 1: Results for the comparison to state-of-the-art (Grover et al., 2019; Cuturi et al., 2019) using the same network architectures averaged over 5 runs. We extend the results table created by Cuturi et al. (2019). Metrics are (EM | EW | EM5).

Method	$n = 3$	$n = 5$	$n = 7$	$n = 9$	$n = 15$
Stoch. NeuralSort	92.0 94.6	79.0 90.7 79.0	63.6 87.3	45.2 82.9	12.2 73.4
Det. NeuralSort	91.9 94.5	77.7 90.1 77.7	61.0 86.2	43.4 82.4	09.7 71.6
Optimal Transport	92.8 95.0	81.1 91.7 81.1	65.6 88.2	49.7 84.7	12.6 74.2
Odd-Even	95.2 96.7 86.1	86.3 93.8 86.3	75.4 91.2 86.4	64.3 89.0 86.7	35.4 83.7 87.6
	$n = 2$	$n = 4$	$n = 8$	$n = 16$	$n = 32$
Odd-Even	98.1 98.1 84.3	90.5 94.9 85.5	63.6 87.9 83.6	31.7 82.8 87.3	1.7 69.1 86.7
Bitonic	98.1 98.1 84.0	91.4 95.3 86.7	70.6 90.3 86.9	30.5 81.7 86.6	2.7 67.3 85.4

Table 2: Results for training on the SVHN data set averaged over 5 runs. Metrics are (EM | EW | EM5).

Method	$n = 2$	$n = 4$	$n = 8$	$n = 16$	$n = 32$
Odd-Even	93.4 93.4 58.0	74.8 85.5 62.6	35.2 73.5 63.9	1.8 54.4 62.3	0.0 36.6 62.6
Bitonic	93.8 93.8 58.6	74.4 85.3 62.1	38.3 75.1 66.8	3.9 59.6 66.8	0.0 42.4 67.7

setting that the n used for evaluation is the same as the n used for training. The evaluation is shown in Table 1. We report results for exact match, correct ranks, and EM5, respectively.

For the odd-even architecture, we compare results for the original $n \in \{3, 5, 7, 9, 15\}$. Our approach outperforms current systems on all metrics and input set sizes. In addition, we extend the original benchmark set sizes by $n \in \{2, 4, 8, 16, 32\}$, allowing for the canonical version of the bitonic sorting network which requires input size of powers of 2. We apply $n \in \{2, 4, 8, 16, 32\}$ to the odd-even as well as the bitonic sorting network. In this direct comparison, we can see that the bitonic and the odd-even architectures perform similar. Notably, the EM and EW accuracies do not always correlate as can be seen for $n = 32$. Here, the EM accuracy is greater for the bitonic network and the EW accuracy is greater for the odd-even network. We attribute this to the odd-even network’s gradients causing swaps of neighbors while the bitonic network’s gradients provide a holistic approach favoring exact matches.

SVHN The results in Table 2 show that the real-world SVHN task is significantly harder than the MNIST task. Again, the performance of odd-even and bitonic is similar. Notably, the EM5 accuracy is largest for the bitonic sorting network at $n = 32$, which demonstrates that the method benefits from longer input sets. Further, for $n \in \{8, 16, 32\}$, the bitonic sorting network marginally outperforms the odd-even sorting network on all metrics.

Scalability We are interested in the effect of training with larger input set sizes n . As the bitonic sorting network is significantly faster and has a lower footprint than odd-even, e.g., for $n = 1024$: 55 vs. 1024 layers, (cf. Ta-

ble 5) we choose the bitonic architecture to evaluate for $n = 2^k, k \in \{5, 6, 7, 8, 9, 10\}$ on the MNIST sorting benchmark, comparing the EM5 accuracy as shown in Table 3. For this evaluation, we consider steepness values of $s \in \{30, 32.5, 35, 37.5, 40\}$ and report the mean, best, and worst over all steepness values for each n . We set α to 0.4 as this allows for stable training with $n > 128$.

To keep the evaluation feasible, we reduce the number of iterations during training to 10^4 , compared to the 10^6 iteration in Tab. 1. Again, we use the Adam optimizer with a learning rate of $10^{-3.5}$.

In the first two columns of Table 3, we show a head to head comparison with the setting in Table 1 with $\alpha = 0.25$ and $\alpha = 0.4$ for $n = 32$. Trained for 10^6 iterations, the EM5 accuracy is 85.4%, while its is 78.2% after 10^4 iterations. Increasing α from 0.25 to 0.4 improves the EM5 accuracy from 78.2% to 80.97%. This shows that already at this scale, a larger α , i.e., a stronger activation replacement trick, can improve the overall accuracy of a bitonic sorting network compared to training with $\alpha = 0.25$.

As the size of training tuples n increases, this also increases the overall number of observed images during training. Therefore, in the left half of Table 3, we consider the accuracy for a constant total of observed images per iteration, i.e., for $n \times$ batch size = 4096 (e.g., for $n = 32$ that results in a batch size of 128, while for $n = 1024$, we can only use a batch size of 4). In the right half of Table 3, we consider a constant batch size of 4.

We see that with increasing n , the accuracy of our model increases even for a constant number of observed images and thus very small batch sizes. This shows that training with larger ordered sets results in better accuracy. It suggests that, if possible, larger n should be prioritized over larger batch sizes and that good results can be achieved by using

Table 3: Results for large n measured using the EM5 metric with fixed number of samples as well as a fixed batch size. Independent of the batch size, for larger n , the model always performs better. Trained for 10^4 iterations and averaged over 10 runs.

α	0.25	0.4	0.4	0.4	0.4	0.4	0.4	0.4	0.4	0.4	0.4	0.4	0.4	0.4
n	32	32	64	128	256	512	1024	32	64	128	256	512	1024	
batch size	128	128	64	32	16	8	4	4	4	4	4	4	4	4
$s = 30$	78.20	79.89	81.25	82.50	82.05	82.50	82.80	71.08	75.88	79.43	81.46	82.98	82.80	
$s = 32.5$	76.98	79.62	81.66	80.15	81.87	82.64	81.63	72.31	75.59	79.71	81.36	82.99	81.63	
$s = 35$	77.45	80.93	81.26	80.72	81.42	81.51	81.15	71.15	75.73	78.81	79.32	82.30	81.15	
$s = 37.5$	76.40	80.02	80.05	81.50	80.05	82.67	80.07	70.69	75.80	79.11	80.64	82.70	80.07	
$s = 40$	77.69	80.97	80.23	81.55	79.75	81.89	81.15	70.20	74.67	78.14	80.06	81.39	81.15	
mean	77.35	80.29	80.89	81.28	81.03	82.24	81.36	71.09	75.53	79.04	80.57	82.47	81.36	
best s	78.20	80.97	81.66	82.50	82.05	82.67	82.80	72.31	75.88	79.71	81.46	82.99	82.80	
worst s	76.40	79.62	80.05	80.15	79.75	81.51	80.07	70.20	74.67	78.14	79.32	81.39	80.07	

Table 4: Ablation Study: Evaluation of the activation replacement trick (ART) at $\alpha = 0.25$ for $n = 4$ and $n = 32$ on the MNIST and the SVHN data set. The displayed metric is EW.

Method	$n = 4$		$n = 32$	
	—	ART	—	ART
Odd-Even (MNIST)	94.5	94.9	61.5	69.1
Bitonic (MNIST)	93.6	95.3	62.8	67.3
Odd-Even (SVHN)	77.3	85.5	28.5	36.6
Bitonic (SVHN)	78.1	85.3	35.0	42.4

Table 5: Runtime, memory requirements, as well as number of layers for sorting n elements including a backward pass of the gradients. Runtime reported for an Nvidia GTX 1070 GPU.

n	Time		Memory		# Layers	
	Odd-Even	Bitonic	Odd-Even	Bitonic	Odd-Even	Bitonic
4	69 ns	52 ns	1KB	840B	4	3
16	1190 ns	759 ns	42KB	28KB	16	10
32	7.4 μ s	3.5 μ s	315KB	152KB	32	15
128	493 μ s	97 μ s	20.2MB	4.1MB	128	28
1024	—	15 ms	10.2GB	549MB	1024	55

the largest possible n for the available data to learn from all available information.

Ablation Study To assess the impact of the proposed activation replacement trick (ART), we evaluate both architectures with and without ART at $\alpha = 0.25$ in Table 4. It shows that the accuracy improves by using the ART for small as well as for large n . For large n , the activation replacement trick has a greater impact on the performance of both architectures.

Runtime and Memory Finally, we report the runtime and memory consumption of differentiable sorting networks in Table 5. We use the native CUDA implementation and measure the time and memory for sorting n input elements including forward and backward pass. It shows that, for a small number of input elements, the odd-even and bitonic sorting networks have around the same time and memory requirements, while for large number of input elements, bitonic is much faster than odd-even.

6. Conclusion

In this work, we presented differentiable sorting networks for training based on sorting and ranking supervision. To this end, we approximated the discrete min and max operators necessary for pairwise swapping in traditional sorting network architectures with their respective differentiable softmax and softmax operators. We proposed an activation replacement trick to avoid the problems of vanishing gradients and well as blurred values. We showed that it is possible to robustly sort and rank even long sequences on large input sets of up to at least 1024 elements. In future, we will investigate differentiable sorting networks for applications such as top- k supervision or learning-to-rank.

References

Ajtai, M., Komlós, J., and Szemerédi, E. An $O(n \log n)$ sorting network. In *Proceedings of the Fifteenth Annual ACM Symposium on Theory of Computing*, STOC '83, New York, NY, USA, 1983. Association for Computing Machinery. URL <https://doi.org/10.1145/800061.808726>.

networks: A new paradigm. Springer Science & Business Media, 2012.

Batcher, K. E. Sorting networks and their applications. In *Proceedings of the April 30–May 2, 1968, spring joint computer conference*, pp. 307–314, 1968.

Bidlo, M. and Dobeš, M. Evolutionary development of growing generic sorting networks by means of rewriting systems. *IEEE Transactions on Evolutionary Computation*, 2019.

Blondel, M., Teboul, O., Berthet, Q., and Djolonga, J. Fast Differentiable Sorting and Ranking. In *International Conference on Machine Learning (ICML)*, 2020.

Ceterchi, R. and Tomescu, A. I. Spiking neural p systems – a natural model for sorting networks. In *Proc. of the Sixth Brainstorming Week on Membrane Computing*, 2008.

Cuturi, M., Teboul, O., and Vert, J.-P. Differentiable ranking and sorting using optimal transport. In *Proc. Neural Information Processing Systems (NIPS)*, 2019.

Goodfellow, I. J., Bulatov, Y., Ibarz, J., Arnoud, S., and Shet, V. Multi-digit number recognition from street view imagery using deep convolutional neural networks. *arXiv preprint arXiv:1312.6082*, 2013.

Govindaraju, N. K., Gray, J., Kumar, R., and Manocha, D. Gputerasort: high performance graphics co-processor sorting for large database management. In *SIGMOD Conference*, 2006.

Gowanlock, M. and Karsin, B. A hybrid cpu gpu approach for optimizing sorting throughput. *Parallel Computing*, 85, 02 2019.

Grover, A., Wang, E., Zweig, A., and Ermon, S. Stochastic Optimization of Sorting Networks via Continuous Relaxations. In *International Conference on Learning Representations (ICLR)*, 2019.

Kingma, D. and Ba, J. Adam: A method for stochastic optimization. In *International Conference on Learning Representations (ICLR)*, 2015.

Knuth, D. E. *The Art of Computer Programming, Volume 3: (2nd Ed.) Sorting and Searching.* Addison Wesley Longman Publishing Co., Inc., USA, 1998. ISBN 0201896850.

LeCun, Y., Cortes, C., and Burges, C. Mnist handwritten digit database. *ATT Labs*, 2, 2010. URL <http://yann.lecun.com/exdb/mnist>.

Lim, C. H. and Wright, S. A box-constrained approach for hard permutation problems. In *International Conference on Machine Learning (ICML)*, 2016.

Metta, V. P. and Kelemenova, A. Sorting using spiking neural p systems with anti-spikes and rules on synapses. In *International Conference on Membrane Computing*, 2015.

Netzer, Y., Wang, T., Coates, A., Bissacco, A., Wu, B., and Ng, A. Y. Reading digits in natural images with unsupervised feature learning. 2011.

Xie, Y., Dai, H., Chen, M., Dai, B., Zhao, T., Zha, H., Wei, W., and Pfister, T. Differentiable top-k with optimal transport. In *Proc. Neural Information Processing Systems (NIPS)*, 2020.

A. Implementation Details

A.1. MNIST

For the MNIST based task, we use the same convolutional neural network architecture as in previous works (Grover et al., 2019; Cuturi et al., 2019). That is, two convolutional layers with a kernel size of 5×5 , 32 and 64 channels respectively, each followed by a ReLU and MaxPool layer; after flattening, this is followed by a fully connected layer with a size of 64, a ReLU layer, and a fully connected output layer mapping to a scalar.

A.2. SVHN

For the SVHN task, we use a network with four convolutional layers with a kernel size of 5×5 and (32, 64, 128, 256) filters, each followed by a ReLU and a max-pooling layer with stride 2×2 ; followed by a fully connected layer with size 64, a ReLU, and a layer with output size 1.

B. Standard Deviation of the Results

Tables 6, 7 and 8 display the standard deviations for the results in this work.

Table 6: Same as Table 1 but with additional standard deviation.

MNIST	$n = 3$	$n = 5$	$n = 7$	$n = 8$	$n = 15$
	95.2 96.7 86.1 ±0.3 ±0.2 ±0.6	86.3 93.8 86.3 ±0.9 ±0.4 ±0.9	75.4 91.2 86.4 ±1.8 ±0.6 ±0.9	64.3 89.0 86.7 ±1.8 ±0.6 ±1.1	35.4 83.7 87.6 ±1.8 ±0.5 ±0.5
MNIST	$n = 2$	$n = 4$	$n = 8$	$n = 16$	$n = 32$
	98.1 98.1 84.3 ±0.3 ±0.3 ±0.9	90.5 94.9 85.5 ±1.2 ±0.6 ±1.5	63.6 87.9 83.6 ±11.6 ±4.2 ±6.1	31.7 82.8 87.3 ±1.5 ±0.5 ±0.5	1.7 69.1 86.7 ±0.5 ±1.5 ±1.0
	98.0 98.0 83.7 ±0.2 ±0.2 ±1.2	91.4 95.3 86.7 ±0.6 ±0.3 ±0.4	69.6 90.0 86.6 ±4.4 ±1.3 ±1.8	30.5 81.7 86.6 ±1.8 ±1.2 ±0.9	2.7 67.3 85.4 ±1.3 ±2.7 ±1.7

Table 7: Same as Table 2 but with additional standard deviation.

SVHN	$n = 2$	$n = 4$	$n = 8$	$n = 16$	$n = 32$
	93.4 93.4 58.0 ±0.4 ±0.4 ±2.0	74.8 85.5 62.6 ±1.2 ±0.7 ±1.1	35.2 73.5 63.9 ±1.2 ±0.5 ±1.1	1.8 54.4 62.3 ±0.8 ±1.6 ±1.6	0.0 36.6 62.6 ±0.0 ±1.5 ±0.8
	93.8 93.8 58.6 ±0.3 ±0.3 ±0.8	74.4 85.3 62.1 ±0.7 ±0.3 ±1.1	38.3 75.1 66.8 ±2.4 ±1.1 ±1.4	3.9 59.6 66.8 ±0.3 ±0.8 ±1.4	0.0 42.4 67.7 ±0.0 ±3.5 ±3.6

Table 8: Same as Table 3 but with additional standard deviation.

α	0.25	0.4	0.4	0.4	0.4	0.4	0.4	0.4	0.4	0.4	0.4	0.4	0.4
n	32	32	64	128	256	512	1024	32	64	128	256	512	1024
batch size	128	128	64	32	16	8	4	4	4	4	4	4	4
$s = 30$	78.20 ±2.35	79.89 ±1.97	81.25 ±1.93	82.50 ±1.09	82.05 ±2.62	82.50 ±1.75	82.80 ±2.27	71.08 ±1.67	75.88 ±2.30	79.43 ±2.35	81.46 ±1.47	82.98 ±2.02	82.80 ±2.27
$s = 32.5$	76.98 ±0.86	79.62 ±3.62	81.66 ±2.42	80.15 ±3.84	81.87 ±2.19	82.64 ±1.60	81.63 ±6.22	72.31 ±2.04	75.59 ±2.05	79.71 ±1.57	81.36 ±1.98	82.99 ±1.67	81.63 ±6.22
$s = 35$	77.45 ±1.64	80.93 ±2.75	81.26 ±2.41	80.72 ±3.89	81.42 ±2.09	81.51 ±2.12	81.15 ±3.12	71.15 ±1.69	75.73 ±2.46	78.81 ±1.36	79.32 ±4.85	82.30 ±1.22	81.15 ±3.12
$s = 37.5$	76.40 ±3.90	80.02 ±1.74	80.05 ±1.93	81.50 ±2.03	80.05 ±3.94	82.67 ±2.21	80.07 ±3.67	70.69 ±2.26	75.80 ±1.22	79.11 ±1.88	80.64 ±2.18	82.70 ±1.66	80.07 ±3.67
$s = 40$	77.69 ±1.54	80.97 ±2.03	80.23 ±3.51	81.55 ±1.97	79.75 ±5.41	81.89 ±2.51	81.15 ±3.31	70.20 ±2.06	74.67 ±2.45	78.14 ±2.49	80.06 ±1.93	81.39 ±1.67	81.15 ±3.31
mean	77.35 ±2.06	80.29 ±2.48	80.89 ±2.48	81.28 ±2.80	81.03 ±3.48	82.24 ±2.03	81.36 ±3.97	71.09 ±2.00	75.53 ±2.10	79.04 ±1.97	80.57 ±2.77	82.47 ±1.71	81.36 ±3.97
best s	78.20 ±3.90	80.97 ±3.62	81.66 ±3.51	82.50 ±3.89	82.05 ±5.41	82.67 ±2.51	82.80 ±6.22	72.31 ±2.26	75.88 ±2.46	79.71 ±2.49	81.46 ±4.85	82.99 ±2.02	82.80 ±6.22
worst s	76.40 ±0.86	79.62 ±1.74	80.05 ±1.93	80.15 ±1.09	79.75 ±2.09	81.51 ±1.60	80.07 ±2.27	70.20 ±1.67	74.67 ±1.22	78.14 ±1.36	79.32 ±1.47	81.39 ±1.22	80.07 ±2.27